Lucas, Cathy H.; Jones, Daniel O.B.; Hollyhead, Catherine J.; Condon, Robert H.; Duarte, Carlos M.; Graham, William M.; Robinson, Kelly L.; Pitt, Kylie A.; Schildhauer, Mark; Regetz, Jim. 2014 Gelatinous zooplankton biomass in the global oceans: geographic variation and environmental drivers. *Global Ecology and Biogeography*, 23 (7). 701-714. 10.1111/geb.12169

# Gelatinous zooplankton biomass in the global ocean: geographic variation and environmental drivers

Cathy H. Lucas[1,#], Daniel O. B. Jones[1], Catherine J. Hollyhead[1,2], Robert H. Condon[3], Carlos M. Duarte[4,5,6], William M. Graham[7], Kelly L. Robinson[7], Kylie A. Pitt[8], Mark Schildhauer[9], Jim Regetz[9]

[1] National Oceanography Centre, University of Southampton Waterfront Campus, European Way, Southampton, SO14 3ZH, UK
cathy.lucas@noc.soton.ac.uk
dj1@noc.ac.uk

[2]Civil, Maritime and Environmental Engineering and Science Unit, University of Southampton, Highfield, Southampton SO17 1BJ, UK.
cjh1g08@soton.ac.uk

[3]University of North Carolina Wilmington, Department of Biology and Marine Biology, 601 S. College Road, Wilmington NC, 28403, USA.
condonr@uncw.edu

[4]Department of Global Change Research, Instituto Mediterráneo de Estudios Avanzados IMEDEA (UIB-CSIC), Esporles, Spain.

[5]The UWA Oceans Institute, The University of Western Australia, M470, 35 Stirling Highway, Crawley WA 6009 Australia.
carlos.duarte@uwa.edu.au

[6]Faculty of Marine Sciences, King Abdulaziz University, P. O. Box 80207, Jeddah 21589 Saudi Arabia

[7]Department of Marine Science, The University of Southern Mississippi, 1020 Balch Blvd., Stennis Space Center, MS 39529, USA.
Monty.Graham@usm.edu
Kelly.L.Robinson@usm.edu

[8]Australian Rivers Institute and Griffith School of Environment, Griffith University, Gold Coast Campus, QLD 4111, Australia.
k.pitt@griffith.edu.au

[9]National Center for Ecological Analysis and Synthesis (NCEAS), 735 State Street, Santa Barbara, CA 93101, USA.
schild@nceas.ucsb.edu
regetz@nceas.ucsb.edu

#Correspondence: Cathy Lucas: National Oceanography Centre, University of Southampton Waterfront Campus, European Way, Southampton, SO14 3ZH, UK.
cathy.lucas@noc.soton.ac.uk

**Article type:** Research paper

**Keywords:** Cnidaria, Ctenophora, Thaliacea, jellyfish blooms, JEDI, global ocean, geographic trends, environmental drivers, macroecology.

**Running title:** Global gelatinous biomass

**Abstract word count:** 299; **Text word count:** 5030

**ABSTRACT**

**Aim:** Scientific debate regarding future trends, and subsequent ecological, biogeochemical and societal impacts, of gelatinous zooplankton (GZ) in a changing ocean is hampered by lack of a global baseline and understanding of the causes of biogeographic patterns. We address this using a new global database of GZ records to test hypotheses relating to environmental drivers of biogeographic variation in the multi-decadal baseline of epipelagic GZ biomass in the world's oceans.

**Location:** Global ocean.

**Methods:** Over 476,000 global GZ data and metadata were assembled from a variety of published and unpublished sources. From this, a total of 91,765 quantitative abundance data from 1934 to 2011 were converted to carbon biomass using published biometric equations and species-specific average sizes. Total GZ, Cnidaria, Ctenophora and Chordata (Thaliacea) biomass was mapped into $5^{o}$ grid cells and environmental drivers of geographic variation tested using spatial linear models.

**Results:** We present JeDI (Jellyfish Database Initiative), a publically accessible database available at http://jedi.nceas.ucsb.edu. We show that: (1) GZ are present throughout the world's oceans; (2) global geometric mean and standard deviation of total gelatinous biomass is $0.53 \pm 16.16$ mg C $m^{-3}$, corresponding to a global biomass of 38.3 Tg C in the mixed layer of the ocean; (3) biomass of all gelatinous phyla is greatest in the subtropical and boreal Northern Hemisphere; and (4) within the North Atlantic, dissolved oxygen, apparent oxygen utilisation and sea surface temperature are the principal drivers of biomass distribution.

**Main conclusions:** JeDI is a unique global dataset of GZ taxa, which will provide a benchmark against which future observations can be compared and shifting baselines assessed. The presence of GZ throughout the world's oceans and across the complete global

spectra of environmental variables indicates that evolution has delivered a range of species able to adapt to all available ecological niches.

## INTRODUCTION

Global climate change and anthropogenic activities are changing the ecology and biogeography of populations inhabiting the world's oceans, with effects likely to be greatest in the high latitudes of the Northern Hemisphere (IPCC, 2007; Jones *et al.*, in press). Empirical evidence indicates that such changes will significantly impact marine ecosystems and associated ecosystem services including fisheries (Cheung *et al.*, 2010). By understanding the relationships between biodiversity and biomass, and their biotic and abiotic drivers, we can begin to predict ecosystem response to future scenarios of climate change, human impact and habitat loss (Cheung *et al.*, 2008; Beaugrand *et al.*, 2010). These relationships are well-established for terrestrial ecosystems (Hendriks *et al.*, 2006; Robinson *et al.*, 2011), but there are far fewer such studies in marine ecosystems owing to the extensive spatiotemporal variability of the oceans and limited availability of robust data for many marine taxa, particularly for the open ocean, deep sea, and the Southern Hemisphere (but see Beaugrand *et al.*, 2010; Tittensor *et al.*, 2010). Additionally, spatial patterns and drivers of biomass are particularly understudied, with fewer established patterns compared with those for biodiversity. Whereas plant biomass (Hese *et al.*, 2005) and production (Field *et al.*, 1998) can be resolved from remotely-sensed products, allowing for global patterns to be examined (Huston & Wolverton, 2009), animal biomass is more elusive. On land, global patterns of animal abundance have been derived to test hypotheses on the allometric scaling of population energy use (Currie & Fritz, 1993), and the drivers of global biomass patterns have also been evaluated for microbial and faunal belowground communities (Fierer *et al.*, 2009). Macroecology, life-history theory and food-web ecology were used to predict global

production and biomass of marine animals (Jennings *et al*., 2008) with highest teleost fish biomass reported for productive, cooler upwellings and mid-latitude shelf seas. Food availability influences spatial patterns of global zooplankton biomass (Hernández-León & Ikeda, 2005) and deep-sea benthic biomass (Wei *et al*., 2010), and bathymetric changes in the biomass of deep-sea benthos have also been characterized at the global scale (Rex *et al.*, 2006). In the more physically-complex and variable sedimentary and rocky intertidal habitats, grain size and wave exposure, respectively are the best predictors of macroinvertebrate biomass (Ricciardi & Bourget, 1999).

Marine zooplankton are crucial for ecosystem function and biogeochemical cycling, linking primary production to higher trophic levels and deep sea communities, and acting as hydroclimatic indicators (Richardson, 2008). Gelatinous taxa within the Cnidaria, Ctenophora, and Chordata (Thaliacea), herein referred collectively as gelatinous zooplankton (GZ), are ubiquitous members of zooplankton communities and important consumers on basal production, both as grazers of phytoplankton (thaliaceans) and predators of zooplankton, fish larvae and other GZ (medusae and ctenophores). They can rapidly reproduce and form blooms under suitable environmental conditions, and have been widely reported to have negative ecological and socio-economic impacts: reducing commercially-harvested fish stocks (Pauly *et al.*, 2009), limiting bioavailable carbon to higher trophic levels and promoting microbially-mediated food webs (Condon *et al.*, 2011), and causing detrimental economic impacts on aquaculture, tourism and coastal infrastructure (Purcell *et al.*, 2007). Nonetheless, GZ provide a vital food source for critically-endangered charismatic species such as the Leatherback turtle *Dermochelys coriacea*, and may even influence their distribution (Houghton *et al*., 2006). Additionally, post-bloom jelly-falls may accelerate the

biological pump and increase carbon sequestration from the upper ocean to the deep sea-floor (Lebrato *et al.*, 2012).

Fossil evidence and evolutionary supposition indicate cnidarians and ctenophores have existed for over 500 million years during which they have independently adapted to the major global climate cycles of warming and cooling and changes in oceanic and atmospheric conditions; in line with paleoecological insights of long-term resilience for terrestrial species (Moritz & Agudo, 2013). A recent study has reported increases in regional and global populations of GZ over decadal timescales (Brotz *et al.*, 2012), although Condon *et al*. (2013) suggest that GZ blooms display predictable periodic or decadal fluctuations rather than a sustained monotonic increase. Insufficient long-term quantitative datasets and the lack of a defined global baseline of gelatinous biomass has been a major limitation to substantiate this concept. Historically, complete estimation of gelatinous biomass has been hindered by sampling difficulties associated with their extreme fragility, seasonal periodicity, physical aggregation and blooming tendencies, paucity of samples from the much of the open ocean and sampling approaches biased toward non-gelatinous taxa. Recent advances have alleviated some of these problems; hence, a composite of data sources on GZ abundance have become available from across the ocean, offering an opportunity to examine the global distribution of biomass for future reference.

The aims of this paper are to (1) define global baselines of carbon biomass for the Cnidaria, Ctenophora, Chordata (Thaliacea) and total GZ (all 3 phyla combined) within the epipelagic ocean; (2) identify geographic trends in global GZ biomass by latitude and Longhurst biogeochemical province; and (3) explore the principal underlying oceanic and environmental drivers of spatial variation in Cnidaria, Ctenophora and Thaliacea mean biomass, with

predictor variables chosen on the basis of published studies. As temperature and food availability are considered to be the most important variables structuring marine ecosystems (Jennings *et al*., 2008; Richardson, 2008) we specifically test *a priori* the following hypotheses relating to biogeographic distribution of gelatinous biomass: 1) GZ biomass is positively correlated with sea surface temperature, and 2) GZ biomass is greater in regions characterised by high primary production. Through these efforts we attempt to take a step towards bridging the current gap between the development of global ecology and biogeography on land and that at sea; a gap that reflects the much lower research effort, about 10%, in the later domain despite the oceans covering 71% of our planet (Hendriks *et al.*, 2006).

## METHODS

### The Jellyfish Database Initiative (JeDI)

JeDI is a scientifically-coordinated global jellyfish database housed at the National Center for Ecological Analysis and Synthesis (Santa Barbara, CA), currently holding over 476,000 quantitative, categorical, presence-absence and presence only data on GZ spanning the past four centuries (Appendix S1) (see Condon *et al*., 2012). GZ data are reported to species level, where identified, but phylum, family and order taxonomic information are reported for all records. Other auxiliary metadata, such as physical, environmental and biometric information relating to the GZ metadata, are included with each respective JeDI entry (Appendix S2). JeDI has also been constructed as a future repository of datasets, and metadata and raw data can be accessed and searched at http://jedi.nceas.ucsb.edu.

### Treatment of JeDI and environmental data

Quantitative numerical abundance data (no. $m^{-3}$) of all GZ taxa in the upper 200 m, collected using a number of sampling gears (Appendix S3), were extracted from JeDI between the years 1934 and 2011. Abundance was converted into biomass (mg C $m^{-3}$) using species, family or group-specific length-mass or mass-mass linear and logistic regression equations (Lucas *et al.*, 2011). Average length measurements for each taxon were taken from the SeaLifeBase database (www.sealifebase.org), with taxonomic verification provided by the Catalogue of Life (www.catalogueoflife.org). As biometric equations are not available for all identified gelatinous taxa, conversions were based on family or class-level comparable lengths, and where the species epithet was not provided, conversions were computed assuming the organism belonged to the same genus as previously identified in the same region. Thirty-three regression equations, representing 18 species of Thaliacea, two Hydrozoa, seven Scyphozoa, one Nuda and five Tentaculata, were used for abundance to biomass conversion of 122 species of GZ recorded in JeDI (Appendix S4).

Maps illustrating the spatial distribution of Cnidaria, Ctenophora, Chordata and total GZ biomass in $5^{o}$ x $5^{o}$ grid cells were produced using ArcGIS v10 ESRI. The minimum number of samples yielding statistically-robust results of the abundance of Cnidaria, Ctenophora, Thaliacea and total GZ biomass in $5^{o}$ grid cells was determined by a bootstrapping exercise whereby ten $5^{o}$ grid cells were chosen randomly from the 20% of regions with the highest number of observations. One hundred replicate bootstrapping simulations were run per cell and the number of observations sampled ranged from 1 - 70 at increasing increments of one without data replacement. Owing to lack of data for the Ctenophora 1 - 20 observations were evaluated. To determine the minimum sample size required to adequately characterize the mean biomass for each cell, relative standard errors (RSE) were compared to the bootstrapping sample size for each bootstrap run (Appendix S5). These comparisons showed

that the RSE decreased rapidly to below 50% after which it stabilised. Using an RSE <50% as the criteria for adequacy and for consistency across all three taxa, the minimum number of observations per grid cell that yielded robust results, while retaining sufficient data for statistical analysis, was 20 data points per grid cell. Consequently, in the North Atlantic (which contains 219 x 5° cells) 47 cells with <20 observations were removed from analysis, leaving a total of 109 out of 156 x 5° cells with any data. Subsequent analysis used $\log_{10}$ transformed data and geometric means, to avoid the effect of extreme observations on the error and further stabilise the variance of data within a cell.

For each grid cell, calculations of the arithmetic mean, standard deviation, geometric mean, geometric standard deviation and coefficient of variation (CV) were computed following the removal of grid cells containing '0' values. CV highlights areas of the global ocean where the extent of variability with respect to the mean is greatest and may be used as an indicator of bloom tendencies defined according to Condon *et al.* (2013). The geometric means were assigned to their appropriate Longhurst province and ocean basin, using the equator as a north-south divide. As data were highly skewed (Table 1), the arithmetic mean was deemed to be an unreliable indication of central tendency and all further synthesis was performed on the geometric mean.

Potential drivers of biomass patterns were chosen based on established hypotheses relating to temperature (sea surface temperature, SST), productivity (primary production, PP; chlorophyll *a*, euphotic depth, apparent oxygen utilisation, AOU), oxygen stress (dissolved oxygen, DO), depth and proximity of coastline (bathymetric depth, distance from coast) that are known to affect biodiversity and biomass in the marine environment (Tittensor *et al.*, 2010) including GZ. Salinity was not considered as many GZ species (particularly

cnidarians), are euryhaline (see Lucas & Dawson, 2014). Furthermore, productivity can be used as an indirect indicator for nutrient availability, as jellyfish generally obtain inorganic nutrients through trophic transfer rather than direct assimilation. This approach encompasses hypotheses about eutrophication causing jellyfish blooms because jellyfish respond to productivity caused by eutrophication rather than the nutrients per se. Environmental parameters were obtained from web-based resources as follows: depth from the National Geophysical Data Centre (NGDC) (http://www.ngdc.noaa.gov/mgg/global/relief/ETOPO2/ETOPO2v2-2006/ETOPO2v2g/), surface chlorophyll *a* and SST from the Aqua MODIS satellite (http://oceancolor.gsfc.nasa.gov/), DO and AOU, as netCDF files, from NODC's World Ocean Atlas 2009, then averaged for the upper 200m of the water column (http://www.nodc.noaa.gov/OC5/WOA09/netcdf_data.html). Euphotic depth data were from NASA GIOVANNI Ocean Color Radiometry - Water Quality Portal (http://gdata1.sci.gsfc.nasa.gov/daac-bin/G3/gui.cgi?instance_id=WaterQuality). Primary production data were annually-integrated PP, averaged for the years 2003-2011, calculated with the VGPM algorithm (Behrenfeld & Falkowski, 1997) from MODIS data. Distance from the coast was calculated from a vector coastline file (http://www.gadm.org/) using the Euclidean Distance tool (spatial analyst extension) in ArcGIS v10. A full summary of GZ biomass, relative contribution of Cnidaria, Ctenophora and Thaliacea to total GZ by abundance and biomass, and average values of environmental parameters for each Longhurst province is given in Appendix S6.

**Statistical analyses and modelling of data**

When modelling the relationship between environmental predictors and response variables, spatial autocorrelation violates the assumptions of traditional statistical approaches (Tittensor

*et al.*, 2010). Spatial autocorrelation extends to the scale of ocean basins. For the Cnidaria, semivariance increased linearly with distance, at least to a distance (lag) exceeding 5500 km, suggesting spatial correlation existed at all scales investigated. For the Thaliacea and Ctenophora a clear sill was reached, where semivariance stopped increasing, and model fits suggested that this occurred at distances of 6670 and 3970 km respectively. This spatial autocorrelation results in deflated estimates of variance and corresponding impacts on inference, among other issues. As a result, variables were modelled and inference conducted using both generalized-linear models (GLM) and multivariate spatial linear models (SLM). Models were developed separately for three taxa (Cnidaria, Ctenophora and Thaliacea), recognising the differing trophic levels and life history characteristics of the groups. Following preliminary data exploration, a $\log_{10}$ transformation of the response variables was selected to homogenise variances and normalise data. GLMs resulted in model residuals that were spatially non-independent for all taxa in global analyses, and therefore SLM were used for final inference.

Spatial analysis was performed using an error-spatial autoregressive (SAR) model (Dormann *et al.*, 2007), which uses maximum-likelihood spatial autoregression. Neighbourhood thresholds between 500 and 10,000 km were tested at 100 km intervals and the optimal neighbourhood size for each taxon was selected by minimising the Akaike information criterion (AIC) for the spatial null model (the model only retaining a spatial autocorrelation term). Backward stepwise elimination of insignificant parameters was then used to determine the minimum adequate model. The importance of individual predictors was assessed through t-tests (GLM) and z-tests (SLM). Models were tested further by separately including quadratic terms and interactions between terms; these did not significantly decrease the deviance of the models compared with the simple models so were not explored further.

Statistical analysis was carried out using the R programming environment and spatial model analyses were carried out using R package "spdep" (Bivand *et al.*, 2008). Owing to sparse data in some areas of the world, the analysis was carried out for the North Atlantic only, an area north of a line between Natal, Brazil, and Bolama, Guinea-Bissau, including the peripheral seas.

## RESULTS

### Global patterns of gelatinous zooplankton biomass

Our quantitative dataset (n = 91,765, $5^{o}$ grid cells = 572) covers 33% of the total ocean area; 43% for the Northern Hemisphere and 23% for the Southern Hemisphere (Fig. 1, Table 2). The global median, and geometric mean and geometric standard deviation of total GZ biomass in the epipelagic ocean for the past 78 years were 0.81 mg C $m^{-3}$, and 0.53 ± 16.62 mg C $m^{-3}$ (Table 1). Total GZ biomass varies >7 orders of magnitude across the ocean, with minimum and maximum geometric means of 2 $x10^{-4}$ and 2.3 x $10^{3}$ mg C $m^{-3}$ recorded within the Indian South Subtropical Gyre and North Pacific Tropical Gyre provinces, respectively. Within the major ocean basins, the geometric mean ranged from 0.01 in the South Indian Ocean to 4.07 mg C $m^{-3}$ in the North Pacific Ocean (Table 2). The highest standard deviation, ±47.89, was recorded from the Arctic.

Our analysis shows that GZ are present across production gradients from eutrophic coastal areas to oligotrophic oceanic subtropical gyres, and across temperature gradients from polar to tropical regions. The top 10% of Longhurst provinces had geometric means of biomass >6 mg C $m^{-3}$: in the Alaska coastal downwelling (11.12 mg C $m^{-3}$), the north-western Atlantic shelf (6.68 mg C $m^{-3}$) and the subarctic, tropical and subtropical North Pacific (6.14 – 14.21 mg C $m^{-3}$) (Appendix S6). Coastal and polar regions in the Northern Hemisphere generally

exhibited the highest average and maximum total GZ biomass values compared to those of the open ocean and Southern Hemisphere (Fig. 1). Maximum total GZ biomass was recorded along the east coast the USA (202,838 mg C $m^{-3}$), the central North Pacific (35,213 mg C $m^{-3}$), the Mediterranean (30,344 mg C $m^{-3}$), the boreal polar region (18,582 mg C $m^{-3}$) and the shelf seas around the British Isles and Norway (14,262 mg C $m^{-3}$) (Fig. 1). While some of these high biomass regions also exhibit high CV particularly around the coasts, indicating the co-occurrence of high biomass and GZ blooms in space and time, on a global scale geometric mean of biomass and CV were negatively correlated ($r_s$ = -0.21, $P < 0.05$, n = 579) suggesting that many low GZ biomass regions can also be highly influenced by occasional blooms and sporadic patchiness. Lowest GZ biomass of <0.01 mg C $m^{-3}$ was in oligotrophic or iron-limited Southern Hemisphere regions, including Western Australia, Brazil, the southern subtropical Indian Ocean and the sub-Antarctic.

When the three taxa are considered separately, the Thaliacea (n = 24,998) and Cnidaria (n = 57,663) are the most widely distributed (Fig. 2), and contributed the most to total GZ biomass and abundance (Appendix S6). Ctenophores (n = 8,757) were sampled primarily from the North Atlantic and to a lesser extent the tropical and subtropical North Pacific (Fig. 2). The global geometric mean and geometric standard deviation of biomass for each phylum were 0.09 ± 20.53 mg C $m^{-3}$ (calculated from 505 grid cells) for the Thaliacea, 4.43 ± 6.89 mg C $m^{-3}$ (511 grid cells) for the Cnidaria and 1.14 ± 24.55 mg C $m^{-3}$ (227 grid cells) for the Ctenophora.

All three taxa displayed similar latitudinal trends in the geometric mean of biomass (Fig. 3). The minimum occurs around 20 - 30°S, then increases with latitude from the equatorial and northern subtropical regions to a peak at around 50 - 60°N. Although data are sparse and

variable for the high latitudes, polar regions supported higher GZ biomass. Similarly, the low number of observations for the Southern Hemisphere makes interpretation of biomass trends south of 30 - 40$^{o}$ difficult to achieve with a high degree of confidence.

**Environmental drivers of Cnidaria, Ctenophora and Thaliacea biomass**

The combination of high spatial autocorrelation, low sample number for the Southern Hemisphere and asymmetry in latitudinal trend between the north and south, may lead to misrepresentation of global patterns. As a result, statistical analyses of environmental drivers for biomass distributions were limited to the North Atlantic where more data are available. Once spatial autocorrelation had been accounted for, significant relationships with Cnidaria, Ctenophora and Thaliacea biomass only existed with DO and AOU. SST ($P < 0.05$) was a significant explanatory variable for biomass of both Thaliacea and Cnidaria. PP ($P < 0.05$) and distance from coast ($P < 0.05$) were specifically related to only Ctenophora and Cnidaria biomass distribution respectively. Cnidarians, ctenophores and thaliaceans were found in a broad range of DO concentrations from 2-8 ml $O_2$ $L^{-1}$, with significant linear trends for all three taxa (Fig. 4 and 5). Significant relationships occurred between AOU and biomass for all three GZ groups ($P < 0.05$) (Table 3). The partial residual plots showed that these relationships, once the other environmental variables had been held constant, were positive for all taxa (Fig. 5). All three GZ taxa were present across the full spectrum of sea surface temperatures between 0 and 28$^{o}$C. The linear trends between average biomass and SST were positive for the Thaliacea ($P < 0.05$) and the Cnidaria ($P < 0.001$), but not significant for the Ctenophora (Fig. 5, Table 3). There was a significant positive relationship between biomass of the Ctenophora and PP ($P < 0.05$) (Fig. 5). Cnidaria biomass also increased with decreasing distance from the coast. There were no significant relationships between biomass and bathymetric depth, euphotic zone depth or chlorophyll *a*.

## DISCUSSION

### Gelatinous biomass in the global ocean

Global estimates of macrozooplankton, and in particular GZ biomass, are extremely rare and are typically accompanied by a number of caveats, mainly relating to uneven spatial coverage of available data across the globe, particularly in the Southern Hemisphere. Our biomass data are significantly more variable than that found by Lynam *et al*. (2011) for the Irish Sea where 62 samples were required to reduce RSE to 5%. None of the 5° grid cells in this study had observed data (not bootstrapped) with an RSE as low as 5%, even those with many thousands of observations. This is most likely a result of the variation in sampling methodologies (Appendix S3) and increased spatial extent of our data from a variety of ocean ecosystems. Moriarty *et al*. (2012) reported a median biomass of 0.19 mg C $m^{-3}$ for macrozooplankton >2 mm sampled from 0 - 350m depth, which is almost twice the depth range used in our analysis (median 0.81 mg C $m^{-3}$ in 0 - 200m depth) and therefore includes regions that sustain lower GZ biomass. Direct comparisons with Lilley *et al.* (2011) are difficult, as their data are expressed as g WW 100 $m^{-3}$, and more significantly, our spatial coverage is more widespread and includes a high proportion of data from the open ocean including the Indian Ocean and the mid-ocean regions of the North Atlantic and Pacific Oceans. Only 31% of the datasets in Lilley *et al*. (2011) are oceanic and many of the other datasets are taken from estuaries, lakes and enclosed seas of the Northern Hemisphere (e.g. Jellyfish Lake in Palau, Honjo Lake in Japan) known to contain significant GZ blooms.

We calculate that cnidarians, ctenophores and thaliaceans contribute 92.0 %, 5.5% and 2.5% to an estimated total global GZ biomass of 38.3 Tg C in the upper 200m of ocean (estimated from our GZ geomean of 0.53 mg C $m^{-3}$ and assuming global ocean area = 361,900,000 $km^2$).

Estimates of global-averaged phytoplankton and zooplankton median biomass are 56 mg C $m^{-3}$ (Boyce *et al*., 2010, where mg Chl *a* is converted to C using median Chl:C of 0.01 according to Behrenfeld *et al.*, 2005) and 4.18 mg C $m^{-3}$ (Strömberg *et al*., 2009: Table A1, where biomass is modelled from primary production and transfer efficiencies), respectively. These order of magnitude differences between successive trophic levels (phytoplankton to zooplankton to GZ) are expected assuming classic food web structure and transfer efficiencies (Strömberg *et al*., 2009). Based on two (thaliaceans) or three (cnidarians, ctenophores) trophic levels, 10% trophic transfer efficiency and 30 - 60 Pg C of primary production available (Watson *et al*., 2013), we estimate that < 0.01 - 12 % of the mean annual global primary production is required to support the estimated global GZ biomass reported in our study.

Our global maps and analyses highlight the truly global distribution of GZ in the world's oceans, from the productive coastal regions where biomass is greatest, to the open ocean and oligotrophic regions. Nevertheless, clear spatial patterns in biomass are evident. While the observed latitudinal trends in Cnidaria, Ctenophora and Thaliacea biomass are in broad agreement with that reported for other macrozooplankton (Moriarty *et al.*, 2012) and crustacean mesozooplankton (see Hernández-León & Ikeda, 2005: Fig. 1; Strömberg *et al.*, 2009: Fig. 2), the differential between the GZ biomass in the Southern and Northern Hemispheres is unclear. It may result from low spatial coverage of quantitative samples, particularly in the Southern Ocean where GZ are known to be abundant, but were unavailable to JEDI. It may reflect zooplankton food availability for GZ predators; Hernández-León & Ikeda (2005) suggested that higher zooplankton biomass at 10 - 20°N compared with the minimal biomass at equivalent latitudes south of the equator was attributed to the productive north-equatorial waters of the Atlantic Ocean. The reduced coastline in the Southern

Hemisphere may be significant for scyphozoan and some hydrozoan jellyfish that require shallow-water hard surfaces for their benthic polyps to inhabit as part of the cnidarian life cycle. Finally, lower human impact (e.g. eutrophication, fishing pressure, contaminant loads) on marine ecosystems in the Southern Hemisphere relative to the Northern Hemisphere (Halpern *et al*., 2008) may also influence GZ biomass, as suggested by Purcell *et al*. (2007).

**Environmental drivers of gelatinous biomass**

Our analyses suggest that the large-scale spatial trends in the baseline distribution of GZ biomass in the Atlantic are significantly related to several environmental variables, particularly SST, DO and primary production. Although data are currently limited, these trends may apply more generally on global scales but interact synergistically with additional environmental variables (e.g. riverine nutrient inputs) on local and regional scales (Condon *et al*., 2013).

In agreement with Lilley *et al*. (2011), we found no significant correlation with chlorophyll *a*, although there was a significant relationship between Ctenophora biomass and primary production. The role of primary production in shaping faunal biomass is a common theme across several taxa and terrestrial and marine ecosystems (Hernández-Leon & Ikeda, 2005: Jennings *et al*., 2008; Fierer *et al*., 2009), and while correlations with PP might be expected as it reflects rates of carbon fixation by the entire autotrophic community that ultimately sustains GZ biomass, it was not a particularly important driver of GZ biomass. The result for chlorophyll *a* is as expected as chlorophyll *a* indicates the net difference between growth and removal processes such as viral lysis and grazing.

There was a broad trend of increasing biomass with increasing DO for all GZ taxa, at the lower end of this scale relatively high GZ biomass was still distributed in regions of persistent low DO and hypoxia. Furthermore, high ctenophore biomass was associated with regions of increased AOU, indicating a connection between GZ biomass and increased community respiration (del Giorgio & Duarte, 2002). These results further indicate that GZ may be able to persist in regions unavailable to other pelagic organisms, such as fish, which are intolerant of low DO conditions (<4 mg $O_2$ $L^{-1}$). They are also consistent with previous studies that suggest several coastal bloom-forming and oceanic GZ species, including *Aurelia* spp., *Chrysaora quinquecirrha*, *Cyanea capillata*, *Mnemiopsis leidyi* and *Pleurobrachia bachei*, tolerate hypoxic (30% air saturation, <2 mg $O_2$ $L^{-1}$) and even severely hypoxic (<0.5 mg $O_2$ $L^{-1}$) conditions (Thuesen *et al*., 2005). Furthermore, extreme abundances of the scyphozoan *Crambionella orsini* have been observed within the Oxygen Minimum Zone (<0.5 mg $O_2$ $L^{-1}$) on the upper slopes off the coast of Oman (Billett *et al.*, 2006). Thus, our findings show a general trend of increasing GZ biomass with increasing DO levels but evidence that high GZ biomass can occur in areas of very low DO. The mechanisms by which GZ can persist under these conditions are not clear and warrant further investigation, but could be related to the unique allometric (e.g. relatively low carbon demand relative to individual size) and intracellular physiological characteristics (e.g. anaerobic pathways) associated with adopting a gelatinous body plan (Pitt *et al*., 2013). GZ have been shown experimentally to exhibit comparatively low oxygen thresholds for hypoxia-driven mortality (Vaquer-Sunyer & Duarte, 2008).

Our analysis for the North Atlantic revealed a significant positive linear relationship between Cnidaria and Thaliacea biomass and SST. This agrees with several other studies that suggest increased cnidarian and thaliacean biomass is associated with warmer SST (e.g. the

Mediterranean, Kogovšek *et al.*, 2010; the North Atlantic, Gibbons & Richardson, 2009), although trends are not universal and species- and geographical-range specific differences in temperature tolerance will drive differences on local and regional scales (see Zhang *et al.*, 2012). In cnidarians, warmer temperatures generally increase rates of asexual reproduction of the benthic polyp phase of the life cycle (Lucas *et al.*, 2012), which could increase production of medusae. For thaliaceans, the mechanisms might also be indirectly driven by SST as generation times and reproductive output are affected by temperature and food availability (Lucas & Dawson, 2014). In Antarctica higher salp abundances are observed during warmer years with low sea ice owing to the higher proliferation of small phytoplankton cells versus diatoms relative to colder years, which likely reflects their ability to efficiently utilise very small cells <2 μm at high filtration rates (Sutherland *et al.*, 2010). Thaliaceans are also prevalent in oligotrophic subtropical gyres where small cells contribute greatly to primary production or have increased in biomass.

The negative relationship of Cnidarian biomass with distance from coast likely reflects their life history. Members of the Class Scyphozoa (e.g. *Aurelia* spp., *Cyanea* spp., *Chrysaora* spp.) dominate cnidarian biomass, the majority of which have a metagenic life cycle that includes a perennial polyp found attached to natural and artificial substrata in shallow coastal habitats. Owing to the short lifespan of most cnidarian medusae, the abundance of the adult population depends on the local polyp populations (Lucas *et al.*, 2012).

**Concluding remarks and future consequences of GZ biomass**

The main drivers of ocean-scale spatial distribution of GZ biomass are SST, DO and AOU; distance from coast and PP are significant drivers only for the Cnidaria and Ctenophora, respectively. Nonetheless, the presence of gelatinous taxa across the complete spectra of

oxygen, temperature and productivity values suggest that the independent evolution of the gelatinous body plan has delivered a range of phyla that are able to adapt to a wide range of ecological niches, demonstrated by the truly global presence of gelatinous zooplankton. Many of the locations that sustain high GZ biomass have experienced increases in SST and reduced DO over the last three decades at rates greater than the global average, which, together with other climate- and anthropogenic-driven impacts (Halpern *et al*., 2008), is expected to continue. Marked shifts in autotrophic assemblages and primary production are also predicted to change with large-scale global processes (Blanchard *et al*., 2012). While the mechanisms are untested, it has been hypothesized that changes in these physical and chemical factors will affect the ecology and global distribution of GZ favouring their future proliferation (Purcell *et al*., 2007).

Our spatial analysis is an essential first step in the establishment of a truly appropriate and uniformly consistent parameterisation of gelatinous presence from which future trends can be assessed and hypotheses tested, particularly those relating multiple regional and global drivers on GZ biomass. It complements the recent temporal meta-analysis of Condon *et al*. (2013) in which global GZ populations (particularly cnidarian medusae) were shown to exhibit oscillations over multi-decadal timescales centred round a baseline. If GZ biomass does increase in the future, particularly in the Northern Hemisphere, this may influence zooplankton and phytoplankton abundance and biodiversity, having a knock-on effect on ecosystem functioning, biogeochemical cycling (Condon *et al.*, 2011; Lebrato *et al*., 2012) and fish biomass (Pauly *et al*., 2009). The continued development of JeDI and a re-analysis several decades from now will enable science to determine whether GZ biomass and distribution alters as a result of anthropogenic climate change.

**ACKNOWLEDGMENTS**

This research was carried out as part of the Global Jellyfish Project sponsored by the National Center for Ecological Analysis and Synthesis (NCEAS). Funding for NCEAS comes from National Science Foundation (NSF) Grant no. DEB-94-21535, from the University of California at Santa Barbara, and from the State of California. We thank Molly Bogeberg for her contribution to the NCEAS Global Jellyfish Project and construction of JeDI. RHC was also supported by NSF Grant no. NSF-OCE 1030149. CJH carried out the data analysis as part of her Master of Research (Ocean Science) project and was supported by the award of a Richard Newitt prize by the University of Southampton. DOBJ was funded for this work as part of the NERC Marine Environmental Mapping Programme (MAREMAP). We would like to thank Derek Tittensor for his help with the analysis.

**REFERENCES**

1. Beaugrand, G., Edwards, M. & Legendre, L. (2010) Marine biodiversity, ecosystem functioning, and carbon cycles. *Proceedings of the National Academy of Sciences USA*, **107**, 10120-10124.
2. Behrenfeld, M.J., Falkowski, P.G. (1997) Photosynthetic rates derived from satellite-based chlorophyll concentration. *Limnology and Oceanography,* **42**, 1-20.
3. Behrenfeld, M.J., Boss, E., Siegel, D.A & Shea, D.M. (2005) Carbon-based ocean productivity and phytoplankton physiology from space. *Global Biogeochemical Cycles*, **19**, GB1006, doi:10.1029/2004GB002299.
4. Billett, D.S.M., Bett, B.J., Jacobs, C.L., Rouse, I.P. & Wigham, B.D. (2006) Mass deposition of jellyfish in the deep Arabian Sea. *Limnology and Oceanography*, **51**, 2077-2083.

5. Bivand, R.S., Pebesma, E.J, Gomez-Rubio, V. (2008) Applied spatial data analysis with R. Springer, New York. 374 pp.

6. Blanchard, J.L., Jennings, S., Holmes, R., Harle, J., Merino, G., Icarus Allen, J., Holt, J., Dulvy, N.K. & Barange, M. (2012) Potential consequences of climate change on primary production and fish production in large marine ecosystems. *Philosophical Transactions of the Royal Society, Series B*, **367**, 2979-2989.

7. Brotz, L., Cheung, W.W.L., Kleisner, K., Pakhomov, E. & Pauly, D. (2012) Increasing jellyfish populations: trends in Large Marine Ecosystems. *Hydrobiologia*, **690**, 3-20.

8. Cheung, W.W.L., Close, C., Lam, V., Watson, R. & Pauly, D. (2008) Application of macroecological theory to predict effects of climate change on global fisheries potential. *Marine Ecology Progress Series*, **365**, 187-197.

9. Cheung, W.W.L., Lam, V.W.Y., Sarmiento, J.L., Kearney, K., Watson, R., Zeller, D. & Pauly, D. (2010) Large-scale redistribution of maximum fisheries catch potential in the global ocean under climate change. *Global Change Biology*, **16**, 24-35.

10. Condon, R.H., Steinberg, D.K., del Giorgio, P.A., Bouvier, T.C., Bronk, D.A., Graham, W.M. & Ducklow, H.W. (2011) Jellyfish blooms result in a major microbial respiratory sink of carbon in marine systems. *Proceedings of the National Academy of Sciences of the United States of America*, **108**, 10225-10230.

11. Condon, R.H., Graham, W.M., Duarte, C.M., Pitt, K.A., Lucas, C.H., Haddock, S.H.D., Sutherland, K.R., Robinson, K.L., Dawson, M.N., Decker, M.B., Mills, C.E., Purcell, J.E., Malej, A., Mianzan, H., Uye, S.-I., Gelcich, S. & Madin, L.P. (2012) Questioning the rise of gelatinous zooplankton in the World's oceans. *Bioscience*, **62**, 160-169.

12. Condon, R.H., Duarte, C.M., Pitt, K.A., Robinson, K.L., Lucas, C.H., Sutherland, K.R., Mianzan, H.W., Bogeberg, M., Purcell, J.E., Decker, M.B., Uye, S-I., Madin, L.P., Brodeur, R.D., Haddock, S.H.D., Malej, A., Parry, G.D., Erikson, E., Quinoñes, J., Acha,

M., Harvey, M., Arthur, J.M. & Graham, W.M. (2103) Recurrent jellyfish blooms are a consequence of global oscillations. *Proceedings of the National Academy of Science of the United States of America*, **110**, 1000-1005.

13. Currie, D.J. & Fritz, J.T. (1993) Global patterns of animal abundance and species energy use. *Oikos*, **67**, 56-68.
14. del Giorgio, P.A. & Duarte, C.M. (2002) Respiration in the open ocean. *Nature*, **420**, 379-384.
15. Dormann, C.F., McPherson, J.M., Araujo, M.B., Bivand, R., Bolliger, J., Carl, G., Davies, R.G., Hirzel, A., Jetz, W., Kissling, W.D., Kuhn, I., Ohlemuller, R., Peres-Neto, P.R., Reineking, B., Schroder, B., Schurr, F.M. & Wilson, R. (2007) Methods to account for spatial autocorrelation in the analysis of species distributional data: a review. *Ecography,* **30**, 609-628.
16. Field, C.B., Behrenfeld, M.J., Randerson, J.T. & Falkowski, P. (1998) Primary production of the biosphere: integrating terrestrial and oceanic components. *Science*, **281**, 237-240.
17. Fierer, N., Strickland, M.S., Liptzin, D., Bradford, M.A. & Cleveland, C. (2009) Global patterns in belowground communities. *Ecology Letters*, **12**, 1238-1249.
18. Gibbons, M.J. & Richardson, A.J. (2009) Patterns of jellyfish abundance in the North Atlantic. *Hydrobiologia*, **616**, 51-65.
19. Halpern, B.S., Walbridge, S., Selkoe, K.A., Kappel, C.V., Micheli, F., Agrosa, C.D., Bruno, J.F., Casey, K.S., Ebert, C., Fox, H.E., Fujita, R., Heinemann, D., Lenihan, H.S., Madin, E.M.P, Perry, M.T., Selig, E.R., Spalding, M., Steneck, R. & Watson, R. (2008) A global map of human impact on marine ecosystems. *Science*, **319**, 948-952.
20. Hendriks, I.E., Duarte, C.M. & Heip, C.H.R. (2006) Biodiversity research still grounded. *Science*, **312**, 1715.

21. Hernández-León, S. & Ikeda, T. (2005) A global assessment of mesozooplankton respiration in the ocean. *Journal of Plankton Research*, **27**, 153-158.

22. Hese, S., Lucht, W., Schmullius, C., Barnsley, M., Dubayah, R., Knorr, D., Neumann, K., Riedel, T. & Schröter, K. (2005) Global biomass mapping for an improved understanding of the $CO_2$ balance – the Earth observation mission Carbon-3D. *Remote Sensing of Environment*, **94**, 94-104.

23. Houghton, J.D.R., Doyle, T.K., Wilson, M.W., Davenport, J. & Hays, G.C. (2006) Jellyfish aggregations and leatherback turtle foraging patterns in a temperate coastal environment. *Ecology*, **87**, 1967-1972.

24. Huston, M.A. & Wolverton, S. (2009) The global distribution of net primary production: resolving the paradox. *Ecological Monographs*, **79**, 343-377.

25. IPCC (Intergovernmental Panel on Climate Change) (2007) Summary for policymakers. In: Solomon, S., Qin, D., Manning, M., Chen, Z. *et al.* (eds) Climate change 2007: the physical science basis. Contribution of Working Group I to the Fourth Assessment Report of the Intergovernmental Panel on Climate Change. Cambridge University Press, New York, p 1–18.

26. Jennings, S., Mélin, F., Blanchard, J.L., Forster, R.M., Dulvy, N.K. & Wilson, R.W. (2008) Global-scale predictions of community and ecosystem properties from simple ecological theory. *Proceedings of the Royal Society B*, **275**, 1375-1383.

27. Jones, D.O.B., Yool, A., Wei, C-L., Henson, S.A., Ruhl, H.A., Watson, R.A. & Gehlen, M. (in press) Global reductions in seafloor biomass in response to climate change. *Global Change Biology*

28. Kogovšek, T., Bogunović, B. & Malej, A. (2010) Recurrence of bloom-forming scyphomedusae: wavelet analysis of a 200-year time series. *Hydrobiologia*, **645**, 81-96.

29. Lebrato, M., Pitt, K.A., Sweetman, A.K., Jones, D.O.B., Cartes, J.E., Oschlies, A., Condon, R.H., Molinero, J.C., Adler, L., Gaillard, C., Lloris, D. & Billett, D.S.M. (2012) Jelly-falls historic and recent observations: a review to drive future research directions. *Hydrobiologia*, **690**, 227-245.

30. Lilley, M.K.S., Beggs, S.E., Doyle, T.K., Hobson, V.J., Stromberg, K.H.P. & Hays, G.C. (2011) Global patterns of epipelagic gelatinous zooplankton biomass. *Marine Biology*, **158**, 2429-2436.

31. Lucas, C.H. & Dawson, M.N. (2014) What are jellyfishes and thaliaceans and why do they bloom? In: Pitt, K.A. & Lucas, C.H. (eds) *Jellyfish Blooms*, Springer. pp 9 - 44. doi: 10.1007/978-94-007-7015-7

32. Lucas, C.H., Pitt, K.A., Purcell, J.E., Lebrato, M. & Condon, R.H. (2011) What's in a jellyfish? Proximate and elemental composition and biometric relationships for use in biogeochemical studies. *Ecology*, **92**, 1704.

33. Lucas, C.H., Graham, W.M. & Widmer, C. (2012) Jellyfish life histories: the role of polyps in forming and maintaining scyphomedusa populations. *Advances in Marine Biology*, **63**, 33-196.

34. Lynam, C.P, Lilley, M.K.S., Bastian, T., Doyle, T.K., Beggs, C.E. & Hays, G.C. (2011) Have jellyfish in the Irish Sea benefited from climate change and overfishing? *Global Change Biology*, **17**, 767-782.

35. Moriarty, R., Buitenhuis, E.T., Le Quéré, C. & Gosselin, M.-P. (2012) Distribution of known macrozooplankton abundance and biomass in the global ocean. *Earth System Science Data Discussions*, **5**, 187-220.

36. Moritz, C. & Agudo, R. (2013) The future of species under climate change. Resilience or decline? *Science*, **341**, 504-508.

37. Pauly, D., Graham, W., Libralato, S., Morissette, L. & Palomares, M.L.D. (2009) Jellyfish in ecosystems, online databases, and ecosystem models. *Hydrobiologia*, **616**, 67-85.

38. Pitt, K.A., Duarte, C.M., Lucas, C.H., Sutherland, K.R., Condon, R.H., Mianzan, H., Purcell, J.E., Robinson, K.R., Uye, S.-I. (2013) Jellyfish body plans provide allometric advantages beyond low carbon content. *PLoS ONE,* **8(8)**, e72683.

39. Purcell, J.E., Uye, S.-I. & Lo, W.-T. (2007) Anthropogenic causes of jellyfish blooms and their direct consequences for humans: a review. *Marine Ecology Progress Series*, **350**, 153-174.

40. Rex, M.A., Etter, R.J., Morris, J.M., Crouse, J., McClain, C.R., Johnson, N.A., Stuart, C.T., Deming, J.W., Thies, R. & Avery, R. (2008) Global bathymetric patterns of standing stock and body size in the deep-sea benthos. *Marine Ecology Progress Series*, **317**, 1-8.

41. Richardson, A.J. (2008) In hot water: zooplankton and climate change. *ICES Journal of Marine Science*, **65**, 279-295.

42. Robinson, L.M., Elith, J., Hobday, A.J., Pearson, R.G., Kendall, B.E., Possingham, H.P. & Richardson, A.J. (2011) Pushing the limits in marine species distribution modelling: lessons from the land present challenges and opportunities. *Global Ecology and Biogeography*, **20**, 789-802.

43. Ricciardi, A. & Bourget, E. (1999) Global patterns of macroinvertebrate biomass in marine intertidal communities. *Marine Ecology Progress Series*, **185**, 21-35.

44. Strömberg, K.H.P., Smyth, T.J., Allen, J.I., Pitois, S. & O'Brien, T.D. (2009) Estimation of global zooplankton biomass from satellite ocean colour. *Journal of Marine Systems*, **78**, 18-27.

45. Sutherland, K.R., Madin, L.P. & Stocker, R. (2010) Filtration of submicrometer particles by pelagic tunicates. *Proceedings of the National Academy of Science of the United States of America*, **107**, 15129-15134.

46. Thuesen, E.V., Rutherford, L.D., Brommer, P.L., Garrison, K., Gutowska, M.A. & Towanda, T. (2005) Intragel oxygen promotes hypoxia tolerance of scyphomedusae. *Journal of Experimental Biology*, **208**, 2475-2482.

47. Tittensor, D.T., Mora, C., Jetz, W., Lotze, H.K., Ricard, D., Berghe, E.V. & Worm, B. (2010) Global patterns and predictors of marine biodiversity across taxa. *Nature*, **466**, 1098-1101.

48. Vaquer-Sunyer, R. & Duarte, C.M. (2008) Thresholds of hypoxia for marine biodiversity. *Proceedings of the National Academy of Sciences of the United States of America,* **105**, 15452–15457.

49. Watson, R., Zeller, D. & Pauly, D. (2013) Primary production demands of global fisheries. *Fish and Fisheries*, doi: 10.1111/faf.12013.

50. Wei, C-L., Rowe, G.T., Escobar-Briones, E., Boetius, A., Soltwedel, T., Caley, M.J., Soliman, Y., Huettmann, F., Qu, F., Yu, Z., Pitcher, C.R., Haedrich, R.L., Wicksten, M.K., Rex, M.A., Baguley, J.G., Sharma, J., Danovaro, R., MacDonald, I.R., Nunnally, C.C., Deming, J.W., Montagna, P., Lévesque, M., Weslawski, J.M., Wlodarska-Kowalczuk, M., Ingole, B.S., Bett, B.J., Billett, D.S.M., Yool, A., Bluhm, B.A., Iken, K. & Narayanaswamy, B.E. (2010) Global patterns and predictions of seafloor biomass using random forests. *PLoS ONE*, **5(12)**, e15323.

51. Zhang, F., Sun, S., Jin, X.S. & Li, C.L. (2012) Associations of large jellyfish distributions with temperature and salinity in the Yellow Sea and East China Sea. *Hydrobiologia*, **690**, 81-96.

## BIOSKETCH

Catherine Hollyhead is currently studying for an EngD at the University of Southampton. Cathy Lucas, Rob Condon, Carlos Duarte, Monty Graham, Kelly Robinson and Kylie Pitt are all members of an NCEAS working group titled "Global expansion of jellyfish blooms: Magnitude, causes and consequences" http://www.nceas.ucsb.edu/projects/12479. Mark Schildauer and Jim Regertz are or were based at NCEAS. Daniel Jones is a researcher in deep-sea biology, with a particular interest in the reservoirs and fate of global gelatinous zooplankton biomass. Author contributions: CHL, CJH, RHC and DOBJ wrote the article; CJH, CHL, RHC & CMD designed the study; DOBJ & CJH analysed the data and prepared the figures; WMG, KLR, KAP, CHL & RHC compiled and assembled the datasets in JeDI, MS & JR provided database technical support at NCEAS. All authors commented on drafts of the manuscript and contributed substantially to revisions.

## SUPPORTING INFORMATION

**Appendix S1**. Maps of the Jellyfish Database Initiative (JeDI) database.

**Appendix S2**. Template used to gather data for entry into the Jellyfish Database Initiative (JeDI) database.

**Appendix S3**. Relative contribution of different sampling methods used to collect quantitative gelatinous zooplankton data.

**Appendix S4**. Published biometric equations and body composition ratios used to convert gelatinous zooplankton species abundance into carbon biomass.

**Appendix S5**. Relative standard errors (RSE) in the mean as a function of the number of observations within a 5° grid cell.

**Appendix S6**. Summary of environmental and gelatinous zooplankton data for each Longhurst province.

## TABLES

**Table 1**. Summary of descriptive statistics of global biomass (mg C $m^{-3}$) of medusae (phylum Cnidaria), ctenophores (phylum Ctenophora) and pelagic tunicates (phylum Chordata), based upon 5° gridded data comprising 91,765 samples taken from the Jellyfish Database Initiative (JeDI). GZ = gelatinous zooplankton; n = number of observations; Mean = geometric mean for biomass and arithmetic mean for all other variables; SD = standard deviation; P(SWilk) = probability of a normal distribution based on a Kolmogorov-Smirnov test; SST = sea surface temperature; DO = dissolved oxygen; AOU = apparent oxygen utilisation.

| Variable | n | Mean ± SD | Maximum | Median | Skewness | P(SWilk) |
|---|---|---|---|---|---|---|
| Total GZ biomass (mg C $m^{-3}$) | 572 | 0.53 ±16.62 | 2292.06 | 0.81 | 17.61 | <0.001 |
| Bathymetric depth (m) | 579 | 3,121 ±1,921 | 6,040 | 3,778 | 0.49 | <0.001 |
| Chlorophyll *a* (mg $m^{-3}$) | 492 | 0.57 ±1.17 | 8.50 | 0.19 | 4.05 | <0.001 |
| SST (°C) | 492 | 20.02 ±9.54 | 32.08 | 24.07 | -0.98 | <0.001 |
| DO (ml $L^{-1}$) | 500 | 4.69 ±1.30 | 7.90 | 4.65 | 0.29 | <0.001 |
| AOU (ml $L^{-1}$) | 495 | 1.32 ±0.78 | 4.17 | 1.06 | 1.16 | <0.001 |
| Euphotic zone depth (m) | 575 | 74.9 ±28.3 | 142.4 | 77.7 | -0.03 | <0.001 |
| Primary production (g C $m^{-2}$ $yr^{-1}$) | 575 | 229.2 ±235.5 | 1593.6 | 154.0 | 2.80 | <0.001 |
| Distance from coast (km) | 579 | 623 ± 621 | 5,878 | 465 | 1.80 | <0.001 |

681

**Table 2**. The geometric mean and geometric standard deviation (SD) of total GZ biomass (mg C $m^{-3}$) for each ocean basin and the Mediterranean Sea (Med). The calculations were performed upon the allocated $5^{o}$ grid cells from the associated Longhurst province with the equator as the north-south divide. For each ocean basin and sea, the number of $5^{o}$ grid cells and the percentage cover this represents, for which quantitative data were available and from which the calculations were made is also shown.

| | Arctic | North Atlantic | South Atlantic | Med | North Pacific | South Pacific | North Indian | South Indian | Southern |
|---|---|---|---|---|---|---|---|---|---|
| Percentage cover | 16% | 80% | 34% | 59% | 39% | 14% | 82% | 39% | 2% |
| Number of grid cells | 46 | 140 | 57 | 10 | 129 | 51 | 49 | 94 | 3 |
| Mean (mg C $m^{-3}$) | 1.38 | 1.61 | 0.17 | 0.22 | 4.07 | 0.37 | 0.13 | 0.01 | 3.63 |
| SD (mg C $m^{-3}$) | 47.98 | 7.53 | 6.60 | 5.48 | 7.00 | 8.58 | 3.11 | 6.72 | 1.76 |

**Table 3**. Generalized-linear model (GLM) and spatial linear model (SLM) results for minimal adequate models using North Atlantic data. Numbers indicate t-values (GLM) or z-values (SLM), asterisks indicate significance of individual predictors: * $p < 0.05$; ** $p < 0.01$; *** $p < 0.001$ and ns is not significant. Coefficients are presented in parentheses. AIC = Akaike information criterion, SST = sea surface temperature, DO = dissolved oxygen, AOU = apparent oxygen utilisation. Moran's I is calculated on the model residuals.

| | Ctenophores | | Thaliaceans | | Cnidarians | |
|---|---|---|---|---|---|---|
| | GLM | SLM | GLM | SLM | GLM | SLM |
| Bathymetric depth | | | | | | |
| Chlorophyll *a* | | | | | | |
| SST | | | (0.17) | (0.13) | (0.06) | (0.05) |
| | | | 5.36*** | 3.76*** | 2.22* | 2.43* |
| DO | (0.29) | (0.24) | (1.68) | (1.28) | (0.55) | (0.58) |
| | 3.60*** | 2.28* | 5.64*** | 3.98*** | 2.71** | 2.82** |
| AOU | (0.46) | (0.34) | (1.63) | (1.24) | (0.46) | (0.49) |
| | 4.27*** | 2.70** | 5.29*** | 4.05*** | 2.09* | 2.20* |
| Euphotic zone depth | | | | | | |
| Primary production | (0.001) | (0.001) | | | | |
| | 2.69** | 2.71** | | | | |
| Distance from coast | | | | | (-0.001) | (-0.001) |
| | | | | | -2.24* | -2.30* |
| $R^2$ (GLM) / Pseudo $R^2$ (SLM) | 0.27 | 0.26 | 0.29 | 0.19 | 0.09 | 0.35 |
| AIC | 144.69 | 143.18 | 179.94 | 176.64 | 103.74 | 104.86 |
| Moran's I | 0.139* | 0.016 ns | 0.193** | 0.022 ns | 0.087 ns | 0.007 ns |

## FIGURE LEGENDS

**Figure 1**. Maps of 5° grid cells data of sampled total gelatinous zooplankton plotted over Longhurst provinces of (a) number of sample observations; (b) maximum biomass (mg C $m^{-3}$); (c) geometric mean of biomass (mg C $m^{-3}$); and (d) coefficient of variation using the arithmetic mean of biomass. Areas where there are no observations are indicated by light blue (sea).

**Figure 2**. Maps of 5° grid cells data of geometric mean biomass (mg C $m^{-3}$) plotted over Longhurst Provinces of (a) Cnidaria; (b) Ctenophora; and (c) Thaliacea. Areas where there are no observations are indicated by light blue (sea).

**Figure 3**. Latitudinal trends of global biomass of (a) Cnidaria; (b) Ctenophora; and (c) Thaliacea. Trends indicated by fit from single-variable linear models (lines with grey area indicating 95% confidence limits). Note log (base 10) scale on y axis.

**Figure 4**. Scatterplots showing significant relationships between biomass of Ctenophora (a-c), Thaliacea (d-f) and Cnidaria (g-j) and environmental variables in the North Atlantic. DO = dissolved oxygen, AOU = apparent oxygen utilisation, SST = sea surface temperature, PP = primary production. Note log (base 10) scale on y axis.

**Figure 5**. Partial residual plots for the predictors of the minimum adequate SLM biomass of Ctenophora (a-c), Thaliacea (d-f) and Cnidaria (g-j) and environmental variables in the North Atlantic. Plots show the individual effects of: DO = dissolved oxygen, AOU = apparent oxygen utilisation, SST = sea surface temperature, PP = primary production, Euphotic depth = euphotic zone depth. A partial residual plot is a plot of $r_i + b_k * i_k$ vs. $x_{ik}$, where $r_i$ is the

ordinary residual for the $i$-th observation, $x_{ik}$ is the $i$-th observation of the $k$-th predictor and $b_k$ is the regression coefficient estimate for the $k$-th predictor. Regression lines indicate partial fits.

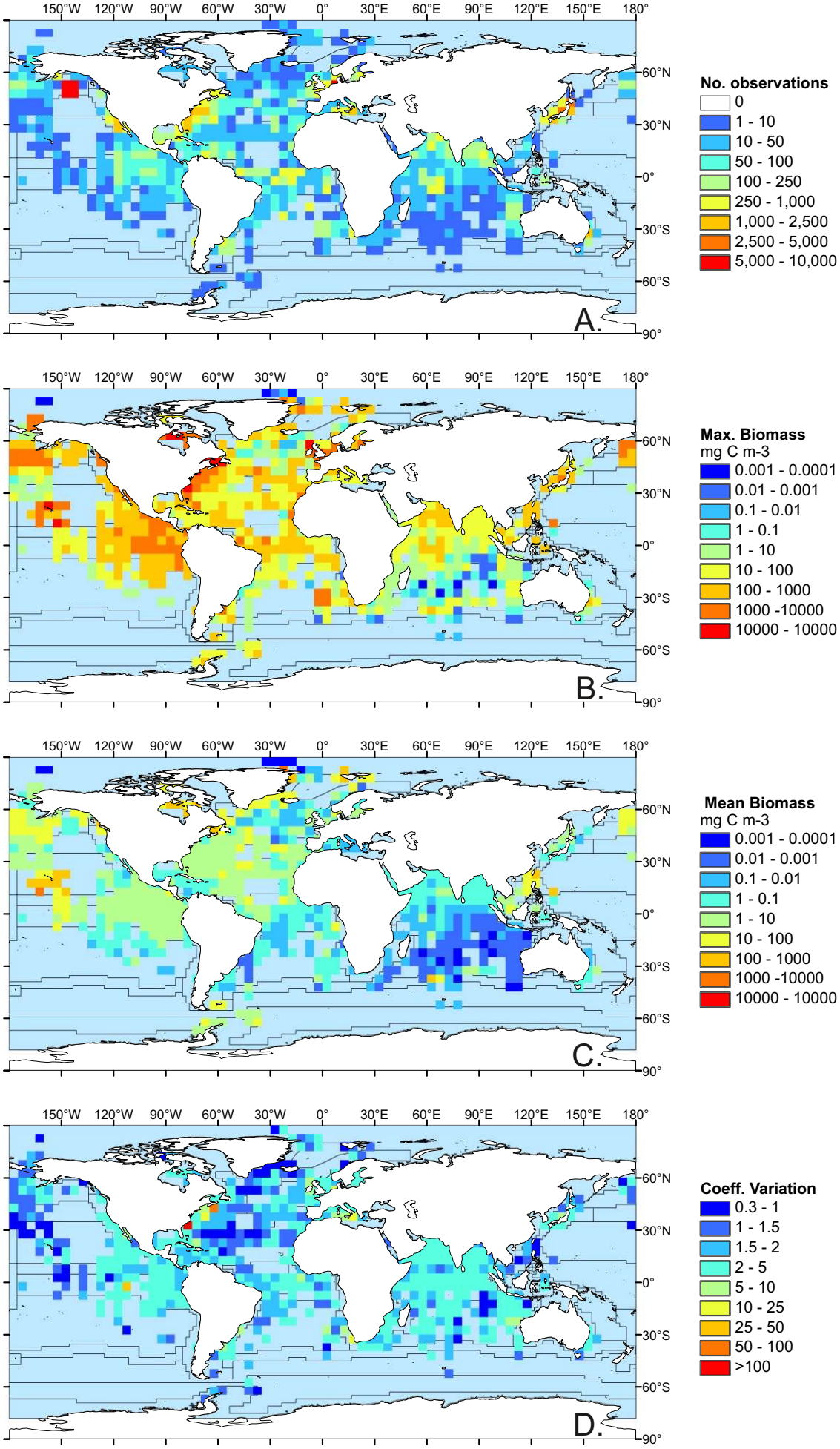
150°W 120°W 90°W 60°W 30°W 0° 30°E 60°E 90°E 120°E 150°E 180°
60°N
30°N
0°
30°S
60°S
90°
A.
No. observations
0
1 - 10
10 - 50
50 - 100
100 - 250
250 - 1,000
1,000 - 2,500
2,500 - 5,000
5,000 - 10,000
B.
Max. Biomass
mg C m-3
0.001 - 0.0001
0.01 - 0.001
0.1 - 0.01
1 - 0.1
1 - 10
10 - 100
100 - 1000
1000 -10000
10000 - 10000
C.
Mean Biomass
mg C m-3
0.001 - 0.0001
0.01 - 0.001
0.1 - 0.01
1 - 0.1
1 - 10
10 - 100
100 - 1000
1000 -10000
10000 - 10000
D.
Coeff. Variation
0.3 - 1
1 - 1.5
1.5 - 2
2 - 5
5 - 10
10 - 25
25 - 50
50 - 100
>100

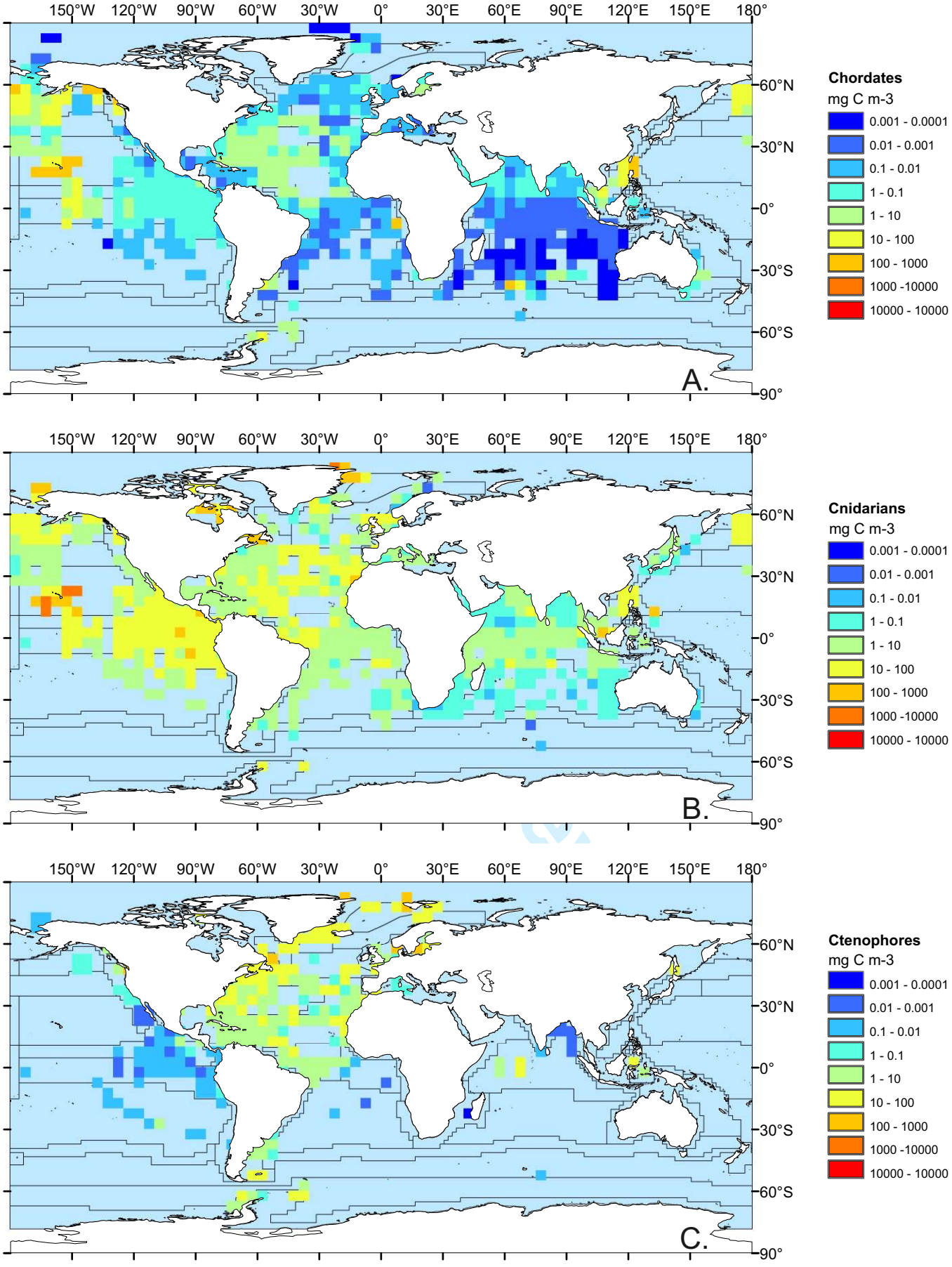
150°W 120°W 90°W 60°W 30°W 0° 30°E 60°E 90°E 120°E 150°E 180°
60°N
30°N
0°
30°S
60°S
90°
A.
Chordates
mg C m-3
0.001 - 0.0001
0.01 - 0.001
0.1 - 0.01
1 - 0.1
1 - 10
10 - 100
100 - 1000
1000 -10000
10000 - 10000
B.
Cnidarians
mg C m-3
0.001 - 0.0001
0.01 - 0.001
0.1 - 0.01
1 - 0.1
1 - 10
10 - 100
100 - 1000
1000 -10000
10000 - 10000
C.
Ctenophores
mg C m-3
0.001 - 0.0001
0.01 - 0.001
0.1 - 0.01
1 - 0.1
1 - 10
10 - 100
100 - 1000
1000 -10000
10000 - 10000